Enterobactin Biosynthesis in *Escherichia coli*: Isochorismate Lyase (EntB) Is a Bifunctional Enzyme That Is Phosphopantetheinylated by EntD and Then Acylated by EntE Using ATP and 2,3-Dihydroxybenzoate†

Amy M. Gehring, Kenneth A. Bradley, and Christopher T. Walsh*

Department of Biological Chemistry and Molecular Pharmacology, Harvard Medical School, 240 Longwood Avenue, Boston, Massachusetts 02115

Received February 27, 1997; Revised Manuscript Received April 30, 1997⊗

ABSTRACT: In *Escherichia coli*, the siderophore molecule enterobactin is synthesized in response to iron deprivation by formation of an amide bond between 2,3-dihydroxybenzoate (2,3-DHB) and L-serine and formation of ester linkages between three such N-acylated serine residues. We show that EntB, previously described as the isochorismate lyase required for production of 2,3-DHB, is a bifunctional protein that also serves as an aryl carrier protein (ArCP) with a role in enterobactin assembly. EntB is phosphopantetheinylated near the C terminus in a reaction catalyzed by EntD with a k_{cat} of 5 min^{-1} and a K_m for apo-EntB of 6.5 μM. This holo-EntB is then acylated with 2,3-DHB in a reaction catalyzed by EntE, previously described as the 2,3-DHB−AMP ligase, with a k_{cat} of 100 min^{-1} and a K_m of <1 μM for holo-EntB. The N-terminal 187 amino acids of EntB (isochorismate lyase domain) are not needed for reaction of EntB with either EntD or EntE as demonstrated by the equivalent catalytic efficiencies of the full-length EntB (residues 1−285) and the C-terminal EntB ArCP domain (residues 188−285) as substrates for both EntD and EntE.

In response to iron deficiency in their environment, many bacterial species synthesize and export low-molecular mass compounds called siderophores which chelate Fe^{III} and are then imported back into the cell to provide iron for metabolic processes. The ability to obtain iron from the environment in this manner has been correlated with the virulence of several bacterial species, including *Escherichia coli* (reviewed in refs 1 and 2). *E. coli*, as well as other species of enteric bacteria, synthesizes the catecholic (dihydroxybenzoyl)serine trilactone, enterobactin (Scheme 1), which is in fact the strongest iron chelator known with a formation constant for ferric enterobactin of 10^{52} M^{-1} (*3*). The synthesis of enterobactin in *E. coli* is among the best studied in terms of genetics, physiology, and biosynthetic enzyme function of all microbial siderophores (reviewed in ref 4). There are six genes, *ent A*−*F*, encoding enzymes of enterobactin biosynthesis in addition to genes for the ferric enterobactin permease (*fep* A−G) and esterase (*fes*) that take the siderophore back up from the environment (*fep*) and release Fe^{III} from the hexacoordinate ligand to allow utilization of the iron (*fes*).

We have previously reported overproduction, purification, and mechanistic studies of the enzymes EntC (*5*), EntB (*6*), and EntA (*7, 8*) which act sequentially to divert carbon from the common aromatic amino acid biosynthetic precursor, chorismate, to 2,3-dihydroxybenzoate via a remarkable series of reactions involving isochorismate (from EntC action on chorismate) and dihydro-2,3-dihydroxybenzoate (produced by EntB, reductively aromatized by EntA) as intermediates (Scheme 2A). In the second phase of enterobactin biosynthesis (Scheme 2B), 2,3-dihydroxybenzoate (DHB)[1] and L-serine are assembled into a trilactone in which three amide linkages (DHB−serine) and three ester linkages (between adjacent serines in the trilactone scaffolding) are fashioned to create the intramolecular hexadentate ligand set in which

Scheme 1

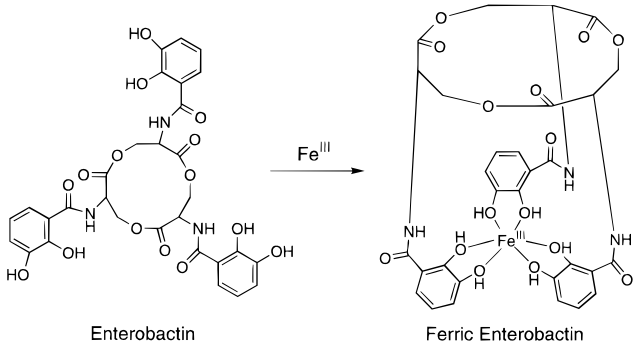

Scheme 2

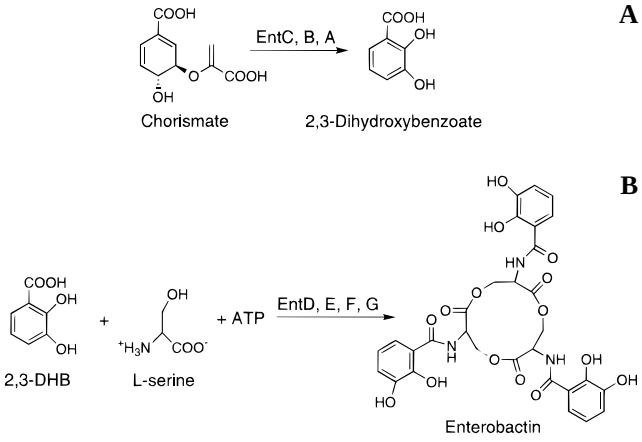

† This work was supported by National Institutes of Health Grant GM20011 to C.T.W. A.M.G. is a Howard Hughes Medical Institute Predoctoral Fellow.

* Author to whom correspondence should be addressed.

⊗ Abstract published in *Advance ACS Abstracts,* July 1, 1997.

S0006-2960(97)00453-4 CCC: $14.00

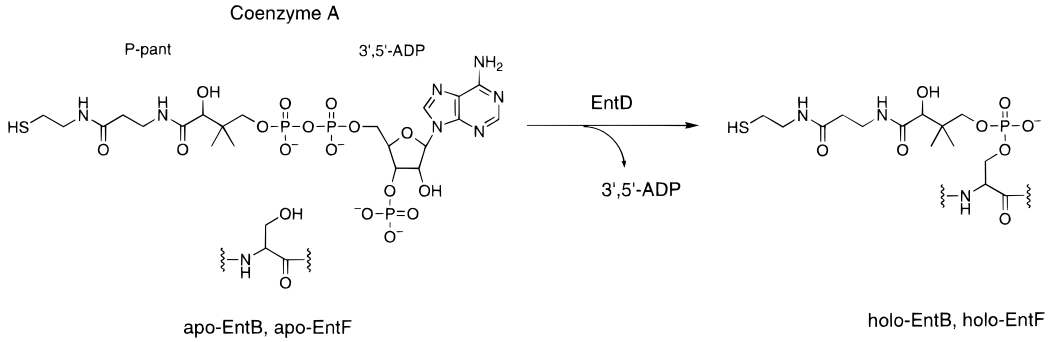

FIGURE 1: Schematic of the phosphopantetheinyl transfer reaction catalyzed by EntD. The P-pant moiety of coenzyme A is attacked by the serine hydroxyl group of apo-EntB or apo-EntF to yield 3′,5′-ADP and holo-EntB or holo-EntF in a Mg^{2+}-dependent reaction.

the three 2,3-DHB catechols chelate the ferric ion. This assembly of enterobactin involves activation by adenylation of both 2,3-DHB by EntE (*9*) and of serine by EntF (*10, 11*) in ATP-cleaving, PP_i-producing reactions.

In addition to the roles delineated for EntE and EntF in the assembly of DHB and serine into enterobactin, genetic analyses proved that there are requirements for EntD (*12*) and EntG (*13*). EntD has recently been identified as a member of the phosphopantetheinyl transferase enzyme family (*14*). Phosphopantetheinyl transferases catalyze conversion of inactive apo forms of acyl carrier proteins (ACP)/peptidyl carrier proteins (PCP) to active holo forms by posttranslational phosphopantetheinylation of a conserved serine side chain in the ACP/PCP domain to give 4′-phosphopantetheine−serine (P-pant−Ser) (Figure 1). EntF has previously been shown to contain phosphopantetheine (*10*), and we have demonstrated that apo-EntF is a substrate for EntD (*14*). As for EntG, no *entG* gene had been identified after complete sequencing of the genetic locus (*7, 15*), and subsequent analysis of *entG* mutants determined that *entG* corresponds to the C terminus of *entB*, the isochorismate lyase gene (Scheme 3) (*16*). It was therefore possible that EntB could be a bifunctional protein with roles both in the synthesis of 2,3-DHB and in the assembly of enterobactin.

In this work, the genetic and biochemical issues surrounding EntB/G are explained by proving that EntB is indeed a bifunctional protein; in addition to its N-terminal isochorismate lyase activity, EntB has a C-terminal apo-ArCP domain (designated ArCP for aryl carrier protein) that undergoes covalent phosphopantetheinylation, most probably at a serine residue located in a consensus sequence, catalyzed by purified EntD. This holo-EntB can then serve as a substrate for EntE which activates DHB as the acyl-AMP derivative and then transfers the acyl fragment onto holo-EntB. Functions are thus now assigned to the EntB, -D, and -E components of the enterobactin synthetase.

MATERIALS AND METHODS

Overproduction and Purification of EntB, EntBΔC, and EntB ArCP. EntB was overproduced from the previously described *E. coli* strain JM105/pFR1 according to the published procedure (*6*). Purification of EntB was similar

Scheme 3

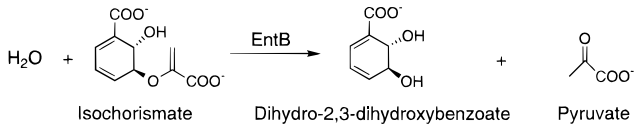

to that described (*6*), but with omission of the gel filtration chromatography step and use of a Q-Sepharose column (2.5 × 10 cm) instead of a Mono-Q 16/10 column. The 30−50% ammonium sulfate pellet was dissolved in 15 mL of 50 mM Tris-HCl (pH 8.0), 2 mM DTT, and 2 mM EDTA (buffer A), dialyzed overnight against 2 × 2 L of buffer A, and then loaded onto the Q-Sepharose column. The column was washed with 100 mL of buffer A (flow rate, 2 mL/min) and the following series of gradients applied: 100 mL of 0 to 25% 1 M KCl (in buffer A), 300 mL of 25 to 55% 1 M KCl, and 100 mL of 55 to 80% 1 M KCl. EntB eluted at approximately 0.4 M KCl. Fractions containing EntB were pooled and concentrated, and the buffer was exchanged for 50 mM Tris-HCl (pH 8.0), 2 mM DTT, and 5% glycerol (v/v) (buffer B). The protein concentration was determined using the calculated extinction coefficient for the absorbance of EntB at 280 nm (51 710 M^{-1} cm^{-1}) (*17*).

EntBΔC was overproduced from the *E. coli* strain JM105/pFR19 (F. Rusnak and C. T. Walsh, unpublished data) in the same manner as EntB. PMSF (0.1 mM) was included in the cell lysis buffer to inhibit proteolysis; however, in two purification attempts, significant amounts of an apparently proteolyzed product were observed (loss of approximately 4 kDa) which could not be removed chromatographically. Purification was as described above for full-length EntB except that the 0−20% ammonium sulfate pellet was dissolved in buffer A and applied to the Q-Sepharose column. The protein concentration was determined by measuring the absorbance at 280 nm and using the calculated extinction coefficient of 40 330 M^{-1} cm^{-1} (*17*).

The gene fragment encoding the EntB ArCP domain (residues 188−285 of full-length EntB) was amplified using PCR methods from the EntB-overexpressing plasmid, pFR1 (*6*). The following primers (Integrated DNA Technologies) were used in the PCR: forward primer, 5′-ATTATAT-CATATGTCCCTGAAATATGTGGCCG-3′; and reverse primer, 5′-TGATGTCCTCGAGTTTCACCTCGCGGG-3′. The forward primer introduced an *Nde*I restriction site (underlined), while the reverse primer introduced an *Xho*I restriction site (underlined) into the PCR product. In addition, the forward primer optimized codon usage for overexpression in *E. coli*. The *Nde*I/*Xho*I-digested PCR product was cloned into the *Nde*I/*Xho*I sites of pET22b (Novagen) to give pET22b-ΔNentB, and this plasmid was

[1] Abbreviations: 2,3-DHB, 2,3-dihydroxybenzoate; 3-HPA, 3-hydroxypicolinate; 4-MHA, 4-methyl-3-hydroxyanthranilate; CoASH, coenzyme A; P-pant, 4′-phosphopantetheine; ACPS, holo-acyl carrier protein synthase; ArCP, aryl carrier protein; ACP, acyl carrier protein; PCP, peptidyl carrier protein; TCA, trichloroacetic acid; BSA, bovine serum albumin; MALDI-TOF, matrix-assisted laser desorption ionization time-of-flight.

used to transform BL21(DE3) *E. coli* cells. Cloning into the *Xho*I site of pET22b adds a C-terminal histidine tag to the overexpressed protein, appending the amino acid sequence LEHHHHHH to the 98 residues of the EntB ArCP fragment. The DNA sequence of pET22b-ΔNentB was confirmed (Dana Farber Molecular Biology Core Facility, Boston).

Cultures of BL21(DE3) pET22b-ΔNentB (2 L, 2× YT media) were grown at 25 °C to an optical density of 0.3. Cultures were induced with 1 mM IPTG and allowed to grow for an additional 5 h, yielding 3.7 g of wet cell paste. Cells were resuspended in 5 mM imidazole, 0.5 M NaCl, and 20 mM Tris-HCl at pH 7.9 (binding buffer) and lysed by two passages through a French pressure cell at 15 000 psi. The lysate supernatant was loaded onto a charged His·Bind column (Novagen) (2.5 × 5 cm) at a flow rate of 0.5 mL/min. The column was then washed with 150 mL of binding buffer (1 mL/min) followed by 90 mL of wash buffer (60 mM imidazole, 0.5 M NaCl, and 20 mM Tris-HCl at pH 7.9) (2 mL/min). The histidine-tagged EntB ArCP was eluted by application of a 90 mL linear gradient of wash buffer to elution buffer (0.5 M imidazole, 0.25 M NaCl, and 10 mM Tris-HCl at pH 7.9) (2 mL/min). The EntB ArCP eluted at approximately 50% elution buffer. EntB ArCP fractions were pooled and dialyzed overnight against 2 L of 50 mM Tris-HCl (pH 8.0) and 2 mM DTT. The protein was then concentrated and the buffer exchanged for buffer B. The protein concentration was determined using the calculated extinction coefficient (at 280 nm) of 19 630 M^{-1} cm^{-1} (*17*). From the 3.7 g of cells used here, about 20 mg of pure EntB ArCP was obtained.

Preparation and Purification of Holo-EntB, Holo-EntB ArCP, and Holo-ACP. Holo-EntB was prepared by incubation of apo-EntB with purified EntD under conditions known to give high levels of conversion of EntB from the apo to the holo form. The following were incubated in a 4 mL volume for 2 h at 37 °C: 10 mM $MgCl_2$, 5 mM DTT, 75 mM Tris-HCl (pH 7.5), 180 μM coenzyme A (CoASH), 25 μM apo-EntB, and 400 nM EntD. After incubation, holo-EntB was purified away from the reaction mixture using the BioCAD SPRINT perfusion chromatography system (PerSeptive Biosystems, Inc.). The reaction mixture was applied to the POROS 20HQ anion-exchange column at a flow rate of 10 mL/min. The column was washed with 4 column volumes of 10 mM Tris and 10 mM Bis-tris propane at pH 8.0 and the holo-EntB eluted with a 30 column volume gradient of 0 to 0.8 M NaCl in the wash buffer. Fractions containing holo-EntB were pooled and dialyzed against 1 L of buffer B.

Holo-EntB ArCP was also prepared by reaction of apo-EntB ArCP with pure EntD. The following reaction mixture (2 mL) was incubated at 37 °C for 2 h: 10 mM $MgCl_2$, 5 mM DTT, 75 mM Tris-HCl (pH 7.5), 500 mM NaCl, 220 μM CoASH, 100 μM apo-EntB ArCP, and 800 nM EntD. The reaction mixture was dialyzed overnight against 1 L of binding buffer. Holo-EntB ArCP was then purified on His·Bind resin (Novagen) according to the manufacturer's suggested procedures. After elution, the holo-EntB ArCP was dialyzed against buffer B. The conversion of apo-EntB ArCP to holo-EntB ArCP was confirmed by MALDI-TOF mass spectral analysis (Biopolymers Facility, Howard Hughes Medical Institute, Harvard Medical School) of the purified product.

Holo-ACP was prepared by reaction of pure apo-ACP with pure ACPS (*18*). The following reaction mixture (1 mL) was incubated at 37 °C for 2 h: 10 mM $MgCl_2$, 25 mM DTT, 75 mM Tris-HCl (pH 8.8), 1.1 mM CoASH, 480 μM apo-ACP, and 1.6 μM ACPS. The reaction mixture was applied to a POROS 20HQ anion-exchange column (10 mL/min); the column was washed with 4 column volumes of 10 mM Tris and 10 mM Bis-tris propane at pH 8.0, and the holo-ACP was eluted with a 25 column volume gradient of 0 to 0.7 M NaCl in the wash buffer. Fractions containing holo-ACP were pooled, concentrated, and exchanged into buffer B. Conversion of apo-ACP to holo-ACP was also confirmed by mass spectral analysis.

Overproduction and Purification of EntD and EntE. EntD was overproduced from strain BL21(DE3)pET28b-entD and purified as previously described (*14*).

EntE was overproduced from strain JM105/pSF105 and purified according to previously published procedures with the following alterations (*9*). For the gel filtration chromatography step, a Sephacryl S-100 column was used (2.5 × 115 cm) at a flow rate of 1 mL/min. For the anion-exchange chromatography step, a Q-Sepharose column was used (2.5 × 10 cm). The column was washed with 100 mL of buffer (25 mM Tris-HCl (pH 8.0), 10 mM $MgCl_2$, and 5 mM DTT) and a 300 mL gradient of 0 to 0.3 M KCl followed by a 100 mL gradient of 0.3 to 1 M KCl applied at a flow rate of 2 mL/min. EntE eluted at approximately 0.25 M KCl. Fractions containing EntE were pooled, concentrated, and exchanged into the following buffer: 25 mM Tris-HCl (pH 8.0), 10 mM $MgCl_2$, 5 mM DTT, and 10% glycerol (v/v). The protein concentration was determined using the calculated extinction coefficient for the absorbance at 280 nm of 55 250 M^{-1} cm^{-1} (*17*).

Assay for Apo- to Holoprotein Conversion by Transfer of [^{3}H]Phosphopantetheine. The radioassay for determination of phosphopantetheinyl transferase activity was carried out as previously described (*14, 18*). Briefly, in a final volume of 100 μL, substrate (EntB, EntBΔC, or EntB ArCP) was incubated with 75 mM Tris-HCl (pH 7.5), 10 mM $MgCl_2$, 25 mM DTT, 240 μM [^{3}H]-(pantetheinyl)-CoASH (specific activity of 43.8 μCi/μmol with 70% of the label in the phosphopantetheine portion of CoASH), and EntD. In addition, 500 mM NaCl was included to relieve substrate inhibition for all of the reactions described in Table 2 and Figure 5. The pH optimum for EntD activity was determined to be pH 7.5 and thus was used. Reaction mixtures were incubated at 37 °C for a specified time and reactions quenched with 800 μL of 10% trichloroacetic acid (TCA) with BSA (375 μg) added as a carrier. Precipitated proteins were pelleted by centrifugation and washed three times with 10% TCA. The protein pellet was dissolved in 1 M Tris base, and the amount of [^{3}H]phosphopantetheine incorporated was quantified by liquid scintillation counting.

For determination of the K_m of EntB and EntB ArCP for EntD, the following conditions were used: 500 mM NaCl, 20 nM EntD, and a 15 min incubation. For determination of the K_m of EntBΔC, the conditions were 500 mM NaCl, 1.6 μM EntD, and a 120 min incubation. The concentration of [^{3}H]CoASH was also decreased to 100 μM to increase the specific activity to 116 μCi/μmol (70% label in phosphopantetheine). As mentioned, the EntBΔC used was not homogeneous, but a mixture of EntBΔC and a putative proteolytic fragment. For the determination of the K_m of CoASH for EntD, the conditions were 500 mM NaCl, 34

μM EntB, 20 nM EntD and, a 15 min incubation; the CoASH used here had a specific activity of 580 μCi/μmol (70% label in phosphopantetheine). All K_m values reported were calculated from at least five different substrate concentrations with assays repeated in triplicate for each substrate concentration.

For the time course assay described in Figure 5, apo-EntB was used at a concentration of 8.4 μM, EntD at 100 nM, and ACPS at 1.5 μM. All other conditions were as described above. For each time point, triplicate assays were performed and data shown are the average of these.

For the autoradiograph shown in Figure 3, 100 μL reaction mixtures were prepared containing 75 mM Tris-HCl (pH 7.5), 10 mM $MgCl_2$, 25 mM DTT, 40 μM [^{3}H]-(pantetheinyl)-CoASH (specific activity of 580 μCi/μmol, 70% label in phosphopantetheine), 800 nM EntD, and 10 μM EntB or EntBΔC or 15 μM EntB ArCP. Reaction mixtures were incubated for 1 h at 37 °C and reactions quenched with TCA as described but with omission of BSA. After washing with TCA, the protein pellet was dissolved in 20 μL of SDS sample buffer and 5 μL of 1 M Tris base. Samples were loaded onto a 12% SDS−PAGE gel and electrophoresed, and the gel was Coomassie-stained and destained. The gel was soaked in Amplify (Amersham) for 25 min, dried, and exposed to film for 3 days.

Assay for the Transfer of [^{14}C]Salicylate to Holo-EntB. The assay used for measuring transfer of salicylate to holo-EntB was as described above for measuring phosphopantetheinyl transfer except that [^{14}C]salicylate was the radiolabeled compound. For the autoradiograph in Figure 7 and the histogram in Figure 8, the reaction was carried out in two parts. For the first reaction, apo-EntB or apo-EntB ArCP was incubated with 75 mM Tris-HCl (pH 8.8), 10 mM $MgCl_2$, 5 mM DTT, 200 μM CoASH, and EntD for 30 min at 37 °C in a volume of 50 μL. For the second reaction, the volume was increased to 100 μL with final concentrations of 75 mM Tris-HCl (pH 8.8), 10 mM $MgCl_2$, 5 mM ATP, 90 μM [^{14}C]salicylate (specific activity of 55.5 μCi/μmol), and EntE with a 20 min incubation at 37 °C. For the histogram in Figure 8, 10 μM apo-EntB, 160 nM EntD, and 100 nM EntE were used and each reaction was performed in triplicate. For the autoradiograph shown in Figure 7, 15 μM apo-EntB or apo-EntB ArCP, 800 nM EntD, and 800 nM EntE were used. Samples were prepared for autoradiography as described in the preceding section with SDS−PAGE on a 4 to 20% Tris-glycine gel (Bio-Rad). This gel was exposed to film for 1 week.

For determination of the kinetic parameters for the reaction of EntE with EntB and EntB ArCP (Table 4), holoproteins were used as substrates (preparation described above). Included in the reaction mixture (50 μL volume) were substrate (holo-EntB or holo-EntB ArCP), 75 mM Tris-HCl (pH 8.8), 10 mM $MgCl_2$, 5 mM DTT, 5 mM ATP, 250 mM NaCl, 500 μM [^{14}C]salicylate (20 μCi/μmol), and EntE. For the assay of EntE with holo-EntB, 2.5 nM EntE was used with an incubation time of 4 min. For the assay of EntE with holo-EntB ArCP, 2.5 nM EntE was used with an incubation time of 2 min. For each K_m determination, seven different substrate concentrations were examined with triplicate assays performed at each substrate concentration. A time course of the transfer of [^{14}C]salicylate to holo-ACP was also done using 14 μM holo-ACP and 500 nM EntE over a time range of 15 min.

Table 1: Comparison of Serine Phosphopantetheinylation Consensus Sequences[a]

E. coli	FAS ACP	D L G A D **S** L
S. violaceoruber	Gra ACP	E L G Y D **S** L
S. rimosus	Otc ACP	A L G Y D **S** L
B. subtilis	SrfB1 PCP	M I G G H **S** L
B. brevis	TycA PCP	S L G G D **S** I
E. coli	EntF PCP	A L G G H **S** L
E. coli	EntB ArCP	D Y G L D **S** V

[a] Abbreviations used in this table: ACP, acyl carrier protein; PCP, peptidyl carrier protein; ArCP, aryl carrier protein; FAS, fatty acid synthase; Gra, granaticin; Otc, oxytetracycline; SrfB1, surfactin synthetase subunit B1; TycA, tyrocidine synthetase subunit A.

Preparation of Samples for Mass Spectral Analysis. Holo-EntB ArCP was prepared by incubation of 40 μg of apo-EntB ArCP with 10 mM $MgCl_2$, 25 mM DTT, 75 mM Tris-HCl (pH 8.8), 200 μM CoASH, and 400 nM EntD in a 100 μL volume at 37 °C for 45 min. Acyl-holo-EntB ArCP was prepared by reaction of 40 μg of apo-EntB ArCP with first 10 mM $MgCl_2$, 25 mM DTT, 75 mM Tris-HCl (pH 8.8), 400 μM CoASH, and 800 nM EntD in a volume of 50 μL at 37 °C for 45 min. An EntE reaction mixture was then added (50 μL) to give a final volume of 100 μL with the following composition: 10 mM $MgCl_2$, 12.5 mM DTT, 75 mM Tris-HCl (pH 8.8), 200 μM CoASH, 5 mM ATP, 500 μM 2,3-DHB or salicylate, 32 μM EntB, 400 nM EntD, and 850 nM EntE. Apo-EntB ArCP, holo-EntB ArCP, and acyl-holo-EntB ArCP were submitted for MALDI-TOF mass spectral analysis (Biopolymers Facility, Howard Hughes Medical Institute, Harvard Medical School).

RESULTS

EntD Catalyzes P-pant Transfer to EntB and a C-Terminal ArCP Fragment. Analysis of the protein sequence of the 285 residues of EntB revealed a potential phosphopantetheinylation site at serine 245 because of similarity to the consensus P-pant sites in other acyl and peptidyl carrier protein (ACP/PCP) domains (Table 1). Given the evidence that the C terminus of EntB corresponds to EntG and is a component of the enterobactin synthetase (*16*), we hypothesized that the C terminus of EntB becomes phosphopantetheinylated and serves as an aryl carrier protein (ArCP) in the assembly of enterobactin. With the recent assignment of EntD as a P-pant transferase (*14*), it was anticipated that EntD would catalyze P-pant transfer to full-length EntB as well as to a C-terminal fragment of it.

Three EntB protein constructs were tested as substrates for EntD: full-length EntB, EntB with the C-terminal 25 amino acids deleted (EntBΔC), and the putative aryl carrier protein domain (EntB ArCP) consisting of the C-terminal 98 amino acids of EntB (residues 188−285) (Figure 2). EntBΔC retains isochorismate lyase activity (F. Rusnak and C. T. Walsh, unpublished data), and the corresponding deletion in the DNA sequence gives an EntB$^+$EntG$^-$ phenotype (*16*). Bounds for the putative ArCP domain were chosen on the basis of observation of an internal ribosome

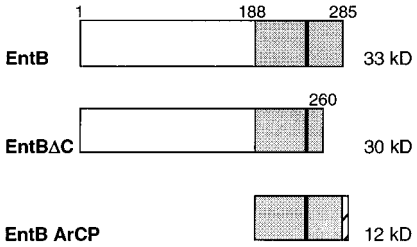

FIGURE 2: Schematic of the EntB protein constructs used in this study. The putative aryl carrier protein (ArCP) domain of EntB is highlighted in gray with the serine phosphopantetheinylation site denoted with a dark line (residue 245). Full-length EntB (residues 1−285, 33 kDa), EntBΔC (residues 1−260, 30 kDa) which has the C-terminal 25 amino acids of EntB deleted, and EntB ArCP (residues 188−285, 12 kDa) consisting of the C-terminal 98 amino acids of EntB succeeded by a hexahistidine tag (hatched box) were all overproduced and purified as described in Materials and Methods.

binding site in *entB* which could direct the synthesis of a C-terminal EntB fragment (11 kDa) composed of the final 98 amino acids of the protein (*16*). EntB (32.5 kDa) and EntBΔC (30 kDa) were overproduced and purified in the native form, while EntB ArCP was overproduced with a C-terminal hexahistidine tag (12 kDa) and purified by nickel chelate chromatography.

The autoradiograph in Figure 3 demonstrates the ability of EntD to transfer [^{3}H]phosphopantetheine to and covalently label both full-length EntB and the EntB ArCP fragment, converting these proteins from their apo to holo forms. When treated with EntD, both full-length EntB (lane 1) and EntB ArCP (lane 3) are strongly labeled with [^{3}H]phosphopantetheine. Transfer of phosphopantetheine to EntBΔC (lane 2) is much less efficient, as indicated by the faintness of labeled EntBΔC in the autoradiograph, thereby corroborating the genetic data. Kinetic parameters for the reaction of EntD with each of these substrates were determined (Table 2). Severe substrate inhibition was observed for the reaction of EntD with either EntB or EntB ArCP. Addition of 0.5 M NaCl to the reaction mixture relieved this substrate inhibition and allowed a more accurate determination of K_m and k_{cat} values (Figure 4). The catalytic efficiency of P-pant transfer to either full-length EntB or the EntB ArCP fragment is comparable with k_{cat}/K_m values of 0.8 and 0.9 μM^{-1} min^{-1}, respectively. Thus, the N-terminal two-thirds of EntB (isochorismate lyase domain) (residues 1−187) do not appear to play a significant role in the interaction of EntD with EntB. Deletion of the C-terminal 25 residues of EntB (EntBΔC), however, results in an approximately 16000-fold decrease in catalytic efficiency.

Previously, we have reported the identification of multiple P-pant transferases in *E. coli*: ACPS (holo-acyl carrier protein synthase) which catalyzes P-pant transfer to the fatty acid apo-ACP, EntD which catalyzes P-pant transfer to the enterobactin synthetase, and o195 of unknown function (*14*). Each P-pant transferase in *E. coli* could catalyze P-pant transfer efficiently only to its cognate apoprotein substrate. For example, EntD was efficient at transferring P-pant to apo-EntF but not to apo-ACP, while ACPS was efficient in catalyzing transfer to apo-ACP but not to apo-EntF (*14*). This specificity in P-pant transfer holds true for EntB as well, as shown in the time course in Figure 5. EntD catalyzes efficient transfer of P-pant from CoASH to apo-EntB, while reaction of this substrate with ACPS is very poor.

EntE Acylates Holo-EntB with 2,3-DHB or Salicylate. Holo-EntB and holo-EntB ArCP formed by reaction with

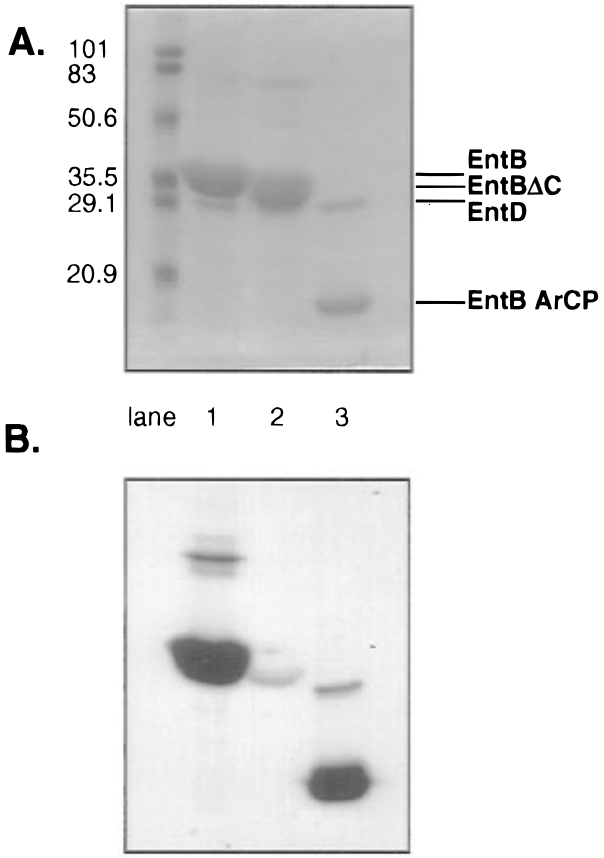

FIGURE 3: Autoradiograph demonstrating EntD-catalyzed incorporation of [^{3}H]phosphopantetheine into the EntB substrates: (A) a Coomassie-stained gel of the reaction mixtures. (B) an autoradiograph of this gel. In each case, substrates were incubated with 40 μM [^{3}H]CoASH (406 μCi/μmol in phosphopantetheine) and 800 nM EntD for 1 h at 37 °C in 100 μL reaction volumes prior to TCA precipitation, 12% SDS-PAGE and autoradiography: lane 1, full-length EntB (10 μM); lane 2, EntBΔC (10 μM); and lane 3, EntB ArCP (15 μM). The radiolabeled band in lanes 1 and 3 with an apparent molecular mass twice that of the EntB and EntB ArCP substrates, respectively, is likely small amounts of holo-EntB and holo-EntB ArCP disulfide dimer which were not reduced by the SDS−PAGE sample buffer.

Table 2: Kinetic Parameters for P-pant Transfer to EntB Substrates Catalyzed by EntD

substrate	k_{cat} (min^{-1})	K_m (μM)	k_{cat}/K_m (μM^{-1} min^{-1})
full-length EntB	5.1	6.5	0.8
EntB ArCP	7.1	7.7	0.9
EntBΔC[a]	0.007	150	5×10^{-5}
coenzyme A	6.4	17	

[a] Purified as a mixture of EntBΔC and a proteolytic fragment.

EntD may then be acylated at the reactive terminal sulfhydryl group of the phosphopantetheine moiety. To synthesize enterobactin, an amide bond must be formed between 2,3-DHB and serine. When amide bonds are formed by nonribosomal peptide synthetases, according to the multiple-carrier thiotemplate mechanism, each residue is activated by a thioester linkage to a 4′-phosphopantetheine cofactor (reviewed in ref 19). For the acylation of serine with DHB, we postulate that holo-EntB is acylated with 2,3-DHB in a reaction catalyzed by EntE while the attacking serine residue is bound as a thioester to EntF (Figure 6). EntE has been shown to catalyze the adenylation of 2,3-DHB as well as its analog salicylate (*9*), and we demonstrate here that EntE also catalyzes the acylation of holo-EntB with 2,3-DHB or

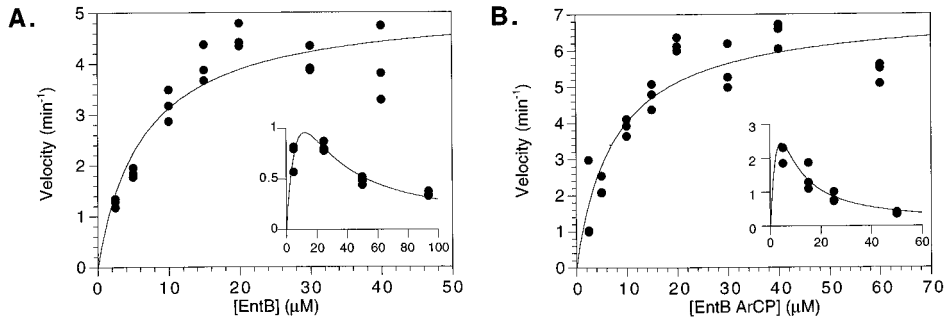

FIGURE 4: Velocity versus substrate concentration plots for the reaction of EntD with (A) full-length EntB and (B) EntB ArCP. The inset shows data from reaction of these EntB substrates with EntD in the absence of salt, while the large panel shows data from the reaction of EntD and the EntB substrates in the presence of 0.5 M NaCl, from which the kinetic parameters in Table 2 were calculated. Addition of NaCl to the reaction mixture largely relieves the severe substrate inhibition observed in its absence. All reactions were carried out at pH 7.5 with 20 nM EntD for 15 min except for reaction of EntB without 0.5 M NaCl (A, inset) which was done at pH 8.8 with 80 nM EntD for 15 min.

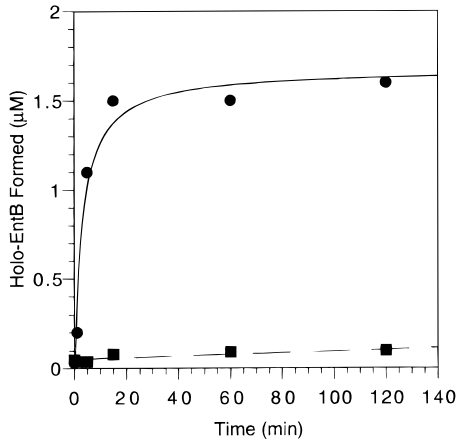

FIGURE 5: Time course of the reaction of apo-EntB (8.4 μM) with EntD (100 nM) (circles) and ACPS (1.5 μM) (squares). Reaction mixtures included 0.5 M NaCl and 240 μM [^{3}H]CoASH (30.7 μCi/μmol in phosphopantetheine), and data shown are an average of three separate reactions. Holo-EntB is formed over this time period in the presence of EntD but is not readily detectable at a 15-fold higher level of ACPS.

salicylate following the adenylation reaction.

The autoradiograph in Figure 7 demonstrates the acylation of holo-EntB (prepared by preincubation with EntD and coenzyme A) with [^{14}C]salicylate in a reaction dependent upon EntE; [^{14}C]salicylate was used as radiolabeled 2,3-DHB is not readily available. Radiolabeled salicylate is covalently incorporated into both full-length holo-EntB (lane 1) and the holo-EntB ArCP fragment (lane 3). Mass spectra were obtained of the 12 kDa EntB ArCP, verifying both phosphopantetheinylation of this protein by EntD and subsequent EntE-mediated acylation with either 2,3-DHB or salicylate (Table 3). Covalent incorporation of salicylate by EntE into EntB requires EntD, CoASH, and ATP as shown in Figure 8.

Kinetic parameters for the EntE-catalyzed transfer of [^{14}C]-salicylate to both full-length holo-EntB and the holo-EntB ArCP fragment were determined (Table 4). Sodium chloride (250 mM) was included in the assay mixture to relieve the substrate inhibition observed in its absence (data not shown). For both holo-EntB and holo-EntB ArCP, the rate of EntE-catalyzed salicyl transfer was approximately 100 min^{-1} with a K_m of $\leq$1 μM for the holo-EntB and holo-EntB ArCP substrates. Because of the low specific activity of the [^{14}C]-salicylate available as well as the low concentrations of holo-EntB and holo-EntB ArCP required for construction of the K_m curves, the difference in the catalytic efficiency of salicyl transfer to holo-EntB versus that to holo-EntB ArCP is not considered significant. Thus, as was observed for EntD-catalyzed phosphopantetheinylation of EntB and its ArCP fragment, deletion of the N-terminal two-thirds of EntB (residues 1−187) does not significantly alter the ability of EntE to catalyze salicyl transfer to holo-EntB ArCP. The rate of release of salicyladenylate from EntE has previously been determined to be approximately 10 min^{-1} (*9*). Thus, the rate of salicyl transfer from EntE to holo-EntB is approximately 10-fold faster than can be accounted for by reaction of free salicyladenylate with holo-EntB and clearly demonstrates that EntE plays a catalytic role in the acylation of holo-EntB.

The ability of EntE to catalyze transfer of salicyladenylate to holo-ACP from *E. coli* was also investigated. Incorporation of [^{14}C]salicylate into holo-ACP (14 μM) was observed if 500 nM EntE was included in the assay mixture compared to the 2.5 nM EntE used to characterize salicyl transfer to holo-EntB and holo-EntB ArCP. A time course of the incorporation of [^{14}C]salicylate into holo-ACP gave a rate of $<$1 min^{-1} (data not shown). Since the rate of salicyl transfer to holo-ACP is less than the rate of release of salicyladenylate into solution by EntE (10 min^{-1}), it is unclear whether EntE is catalyzing transfer of salicylate to holo-ACP or if holo-ACP is acylated nonenzymatically by salicyadenylate released into solution.

DISCUSSION

In this study, we have demonstrated that EntB is a bifunctional enzyme with an N-terminal isochorismate lyase domain and a C-terminal aryl carrier protein domain. EntD phosphopantetheinylates the EntB ArCP domain to yield holo-ArCP. The holo-EntB ArCP domain is then acylated with 2,3-DHB in a reaction in which EntE catalyzes the activation of 2,3-DHB by adenylation as well as the transfer of DHB to the phosphopantetheine cofactor of holo-EntB. This discovery of a function for EntB in the enterobactin synthetase reconciles the genetic and biochemical data indicating that *entB* (isochorismate lyase) and *entG* (enterobactin synthetase component) are one and the same. In a study by Staab and Earhart (*16*), *entG* mutations were localized to the C terminus of EntB, and it was shown that antibodies directed against EntB could completely inhibit activity of the enterobactin synthetase. Here, the function of EntB in the enterobactin synthetase is identified; 2,3-DHB, previously activated as the acyladenylate by EntE, is activated by thioester linkage to the C-terminal P-pant moiety

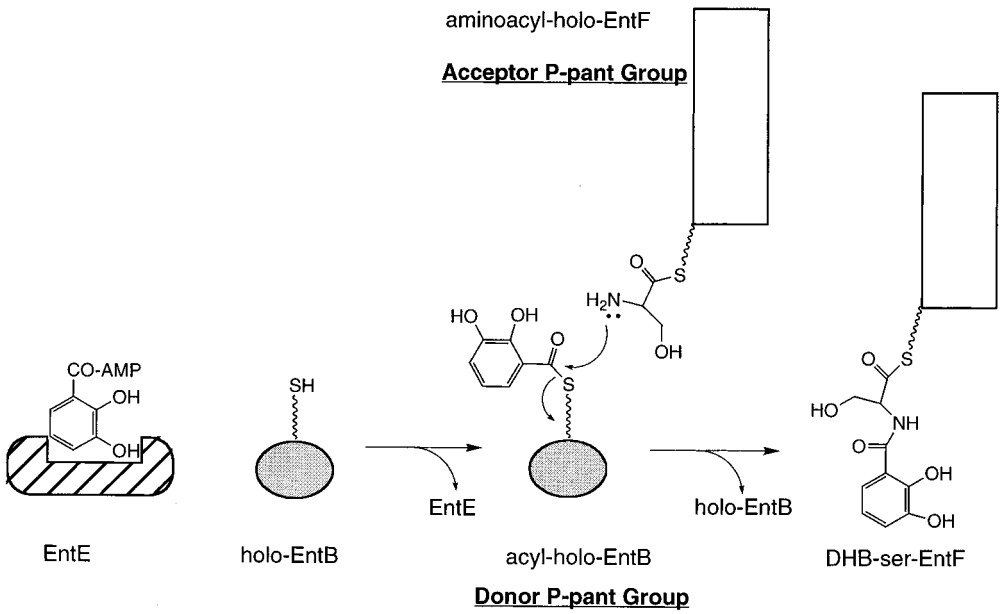

FIGURE 6: Schematic showing the proposed amide bond-forming reaction between 2,3-DHB thioesterified to holo-EntB and serine thioesterified to holo-EntF. The phosphopantetheinylation of EntB by EntD has been demonstrated in this study as well as the acylation of holo-EntB catalyzed by EntE using either 2,3-DHB adenylate or salicyladenylate as the substrate. Previously, the phosphopantetheinylation of apo-EntF by EntD has been shown (*14*) as well as the ability of EntF to form seryl-AMP (*10, 11*). We expect that EntF will catalyze formation of a thioester linkage between the seryl group and its P-pant moiety and propose that acylated holo-EntB will serve as the donor P-pant group and aminoacylated holo-EntF as the acceptor P-pant group in the amide bond-forming reaction between 2,3-DHB and L-serine, resulting in formation of a DHB−Ser−EntF intermediate.

of EntB in a transfer reaction catalyzed by EntE in preparation for amide bond formation with L-serine. As a side note, EntB is also hereby identified as the unknown 35 kDa protein which is labeled when *panD*$^-$ cells are grown in the presence of [^{3}H]-β-alanine under iron-limiting conditions (*10, 20*).

EntD has recently been identified as a P-pant transferase and shown to catalyze P-pant transfer to apo-EntF (*14*). This study shows that apo-EntB is also a substrate for EntD. The presence of at least two P-pant moieties in the multicomponent enterobactin synthetase suggests the following. The P-pant groups on holo-EntB and holo-EntF may serve as the donor and acceptor P-pant group, respectively, in the amide bond-forming reaction between 2,3-DHB and L-serine (Figure 6). We expect that EntF, which has been shown to catalyze the adenylation of L-serine (*10, 11*), will also catalyze the formation of a thioester linkage between its covalently linked phosphopantetheine moiety and the activated seryl group. The amine group of serine now thioesterified to the acceptor P-pant group of holo-EntF will then attack the 2,3-DHB moiety thioesterified to the donor P-pant group of holo-EntB, resulting in amide bond formation and a DHB−Ser−*S*−pantetheinyl-EntF intermediate. Bryce and Brot (*21*) reported isolation of such an enzyme-linked DHB−Ser intermediate from assay of partially purified enterobactin synthetase components. Finally, three such DHB−Ser intermediates will be joined by ester linkages to complete the synthesis of enterobactin by an as yet unknown mechanism. Interestingly, a putative elongation domain has been identified in the N terminus of EntF which may be important for condensation of 2,3-DHB thioesterified to the aryl carrier protein domain of holo-EntB and serine thioesterified to the peptidyl carrier protein domain of holo-EntF (*22*).

Proteins homologous to the enterobactin synthetase components described here have been implicated in the biosynthesis of several other microbial siderophores, namely yersiniabactin produced by *Yersinia* species (*23, 24*) and anguibactin produced by *Vibrio anguillarum* (*25*) (Figure 9). The structures of yersiniabactin (*26, 27*) and anguibactin (*28*) contain salicylate and 2,3-DHB, respectively, in an amide linkage to a cysteine residue (subsequently cyclized to a thiazoline ring). The *V. anguillarum* protein AngR, required for anguibactin biosynthesis, can complement a mutation in the *E. coli entE* gene (*25*). YbtE has been identified in *Yersinia pestis* with 61% similarity and 42% amino acid identity to EntE (*24*). We therefore expect that AngR and YbtE can activate 2,3-DHB and salicylate, respectively, to the acyladenylate and subsequently catalyze the transfer of this aryl acyl group to an aryl carrier protein domain.

A large class of peptidolactone antibiotic molecules produced by *Streptomyces* species resemble enterobactin in that a threonine or serine residue at the N terminus of a short peptide is acylated with an aromatic or heteroaromatic carboxylic acid and an ester linkage is formed between the hydroxyl group of this threonine or serine and the C-terminal amino acid of the peptide (reviewed in ref 29); examples of such cyclic peptidolactones include actinomycin D and pristinamycin I (Figure 9). The biosynthesis of enterobactin may thus also provide a model for the enzymatic synthesis of these peptidolactone antibiotics. The work reported here may help address two important questions about the initiation of peptidolactone synthesis. (1) How many P-pant moieties are required to catalyze amide bond formation between the aryl group and the first amino acid residue of the peptide, and (2) does the aromatic acid-activating enzyme (the acyl AMP ligase) have any role in initiating peptide synthesis?

The purification of three components of the pristinamycin synthetase has recently been accomplished (*30*), and of these, the *snbA* and the *snbC* genes have been sequenced which encode the 3-hydroxypicolinic acid (3-HPA):AMP ligase and the pristinamycin synthetase 2, respectively (*31*). SnbA is an EntE homolog, while SnbC activates as thioesters the first two amino acids of the peptide, threonine and aminobutyric acid. Two phosphopantetheinylation consensus sequences were noted in the SnbC sequence, following the threonine

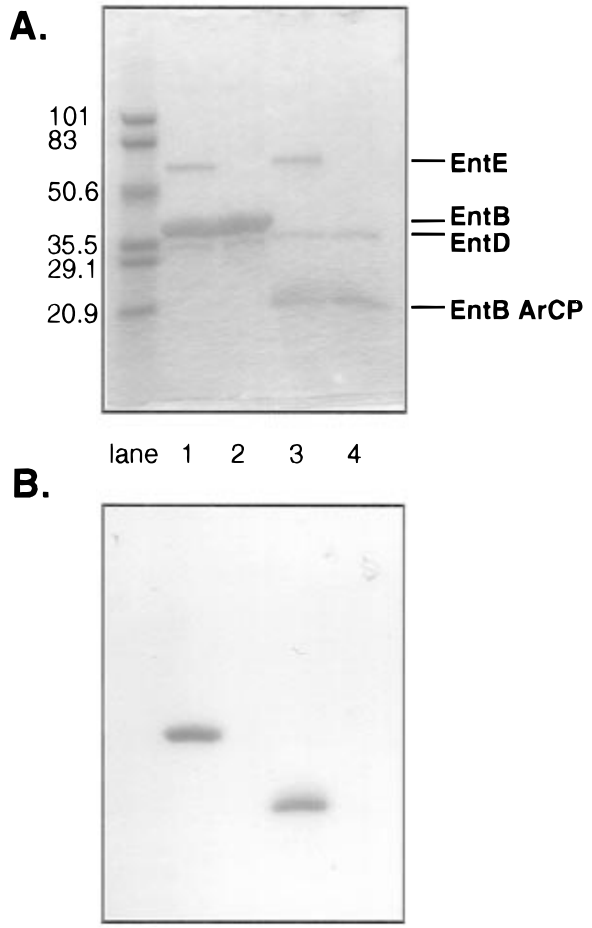

FIGURE 7: Autoradiograph demonstrating the EntE-catalyzed acylation of holo-EntB and holo-EntB ArCP with [^{14}C]salicylate: (A) a Coomassie-stained gel of the reaction mixtures and (B) an autoradiograph of this gel. In each case, substrates were preincubated with EntD (1.6 μM) and coenzyme A (200 μM) for 30 min at 37 °C (50 μL). The acylation reaction mixture was then added (50 μL) which gave final concentrations of 5 mM ATP, 90 μM [^{14}C]salicylate (55.5 μCi/μmol), and in some cases 800 nM EntE with incubation for an additional 20 min before TCA precipitation, SDS−PAGE on a 4 to 20% gradient gel, and autoradiography: lane 1, full-length EntB (15 μM) with EntE; lane 2, full-length EntB (15 μM) without EntE; lane 3, EntB ArCP (15 μM) with EntE; and lane 4, EntB ArCP (15 μM) without EntE.

Table 3: Mass Spectral Data Demonstrating the Phosphopantetheinylation and Acylation of EntB ArCP

EntB ArCP	molecular mass (Da)	
	calculated	observed
apo	12 018[a]	12 024[b]
holo	12 357	12 371[c]
acyl-holo (2,3-DHB)	12 494	12 495[d]
acyl-holo (salicylate)	12 477	12 531

[a] EntB ArCP minus the N-terminal methionine. [b] Average of two determinations: 12 041 and12 007 Da. [c] Average of two determinations: 12 397 and 12 346 Da. [d] Average of two determinations: 12 488 and 12 503 Da.

and aminobutyric acid-activating domains. However, no P-pant consensus sequence was noted at the N terminus of SnbC which could be occupied by a 3-HPA thioester. This prompted the authors to propose the following model for the formation of an amide bond between 3-HPA and threonine. The P-pant moiety succeeding the Thr-adenylating domain would initially be thioesterified to the 3-HPA acyl group which would then be transferred to a waiting site. At this time, a new thioester bond would be formed between

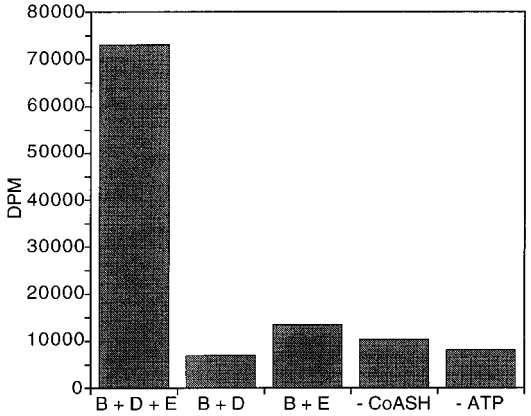

FIGURE 8: Histogram of the incorporation of [^{14}C]salicylate into holo-EntB demonstrating the requirement of EntE, EntD, coenzyme A, and ATP for the occurrence of this reaction. All reaction mixtures (100 μL) included 90 μM [^{14}C]salicylate (55.5 μCi/μmol), 10 μM EntB, 100 μM coenzyme A, 5 mM ATP, 160 nM EntD, and 100 nM EntE unless omitted as indicated. Each data point represents an average of three separate determinations.

Aryl Acyl AMP-Ligases Analogous to EntE

Enzyme		Aromatic Acid Activated	Natural Product	Function	Ref.
EntE	59 kD	2,3-Dihydroxybenzoate	Enterobactin	siderophore	*9*
AngR	118 kD	2,3-Dihydroxybenzoate	Anguibactin	siderophore	*25, 36*
YbtE	57 kD	Salicylate	Yersiniabactin	siderophore	*24*
SnbA	61 kD	3-Hydroxypicolinate	Pristinamycin I	antibiotic	*30,31*
ACMS I	45 kD	4-Methyl-3-hydroxy anthranilate	Actinomycin	antibiotic	*32,34*

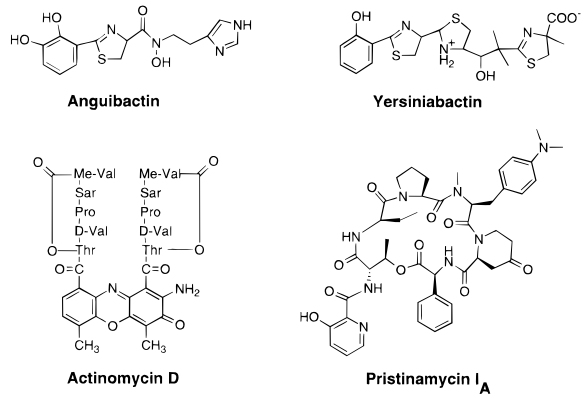

FIGURE 9: List of enzymes with a described or proposed function analogous to that of EntE, an aryl acyl AMP ligase. These enzymes are involved in the biosynthesis of the depicted siderophore or antibiotic molecules anguibactin, yersiniabactin, pristinamycin I_A, and actinomycin D: Sar, sarcosine (*N*-methylglycine); and Me-Val, *N*-methyl-L-valine.

Table 4: Kinetic Parameters for the EntE-Mediated Transfer of Salicylate to Holo-EntB

substrate	k_{cat} (min^{-1})	K_m (μM)	k_{cat}/K_m (μM^{-1}min^{-1})
holo-EntB	100	0.4	250
holo-EntB ArCP	130	1.2	110

threonine and the P-pant moiety with amide bond formation proceeding between the thioesterified threonine and the 3-HPA group held at the yet to be characterized waiting site (*31*). However, if pristinamycin I biosynthesis follows the enterobactin precedent detailed in this work, the simpler explanation for the lack of a third P-pant moiety in SnbC which would form a thioester with 3-HPA is that this P-pant

moiety exists on a distinct aryl carrier protein analogous to EntB. Formation of the amide bond between 3-HPA and threonine would occur in trans between donor and acceptor P-pant groups on the aryl carrier protein and SnbC instead of in cis solely on the SnbC polypeptide. Indeed, the first 520 amino acids of EntF and SnbC are highly similar with about 30% identity which includes a putative elongation motif (*22*).

Components of the actinomycin synthetase have also been purified and characterized (*32*−*35*). ACMSI is a 4-methyl-3-hydroxyanthranilic acid (4-MHA)-AMP ligase (*34*), while ACMSII is responsible for activating threonine and valine as thioesters (*33*). The initiation of peptide synthesis by ACMSI and ACMSII was investigated with observation of the formation of enzyme-bound *p*-toluylthreonine (*p*-toluene is a 4-MHA analog) dependent on the presence of both ACMSI and ACMSII (*35*). The authors hypothesized that ACMSII reacts directly with the toluyladenylate, released into solution by ACMSI, to initiate peptide synthesis because *p*-toluylthreonine could be formed in the absence of ACMSI when chemically synthesized *p*-toluyladenylate was included in the reaction mixture. However, in enterobactin biosynthesis, we have shown that EntE not only catalyzes adenylation of 2,3-DHB/salicylate but also catalyzes formation of a thioester bond between the activated acyl group and the P-pant group of an aryl carrier protein. Rates of thioester formation between salicylate and holo-EntB (100 min^{-1}) were much too fast to be accounted for by reaction of holo-EntB with salicyladenylate released to the solution. In fact, the rate of 4-MHA−AMP formation catalyzed by ACMSI at 0.44 min^{-1} (*34*) is strikingly similar to the slow rate of release of 2,3-DHB adenylate from EntE at 0.41 min^{-1} (*9*). We anticipate that ACMSI may have a greater role, e.g. catalysis of aryl acyl-S-protein formation, in the initiation of actinomycin biosynthesis than has previously been reported. In this study, we have provided new information about the roles of EntD, EntB, and EntE in the enterobactin synthetase. Principles learned from enterobactin biosynthesis may be applicable to the biosynthesis of a variety of other peptidolactone and siderophore molecules. Work to determine the role of EntF in the enterobactin synthetase is ongoing with the ultimate goal of reproducing complete enterobactin biosynthesis *in vitro* from pure synthetase components.

ACKNOWLEDGMENT

We thank Roger S. Flugel for providing pure apo-ACP. We also thank Michelle Obenauer of the Howard Hughes Medical Institute Biopolymer Facility (Harvard Medical School) for performing the mass spectral analyses and the Dana Farber Molecular Biology Core Facility (Boston, MA) for DNA sequence analysis.

REFERENCES

1. Griffiths, E. (1987) in *Iron and Infection: Molecular, Physiological and Clinical Aspects* (Bullen, J. J., and Griffiths, E., Eds.) pp 1−25, John Wiley & Sons, Chichester, Great Britain.
2. Payne, S. M. (1988) *CRC Crit. Rev. Microbiol. 16*, 81−111.
3. Harris, W. R., Carrano, C. J., Cooper, S. R., Sofen, S. R., Avdeef, A. E., McArdle, J. V., and Raymond, K. N. (1979) *J. Am. Chem. Soc. 101*, 6097−6104.
4. Walsh, C. T., Liu, J., Rusnak, F., and Sakaitani, M. (1990) *Chem. Rev. 90*, 1105−1129.
5. Liu, J., Quinn, N., Berchtold, G. A., and Walsh, C. T. (1990) *Biochemistry 29*, 1417−1425.
6. Rusnak, F., Liu, J., Quinn, N., Berchtold, G. A., and Walsh, C. T. (1990) *Biochemistry 29*, 1425−1435.
7. Liu, J., Duncan, K., and Walsh, C. T. (1989) *J. Bacteriol. 171*, 791−798.
8. Sakaitani, M., Rusnak, F., Quinn, N. R., Tu, C., Frigo, T. B., Berchtold, G. A., and Walsh, C. T. (1990) *Biochemistry 29*, 6789−6798.
9. Rusnak, F., Faraci, W. S., and Walsh, C. T. (1989) *Biochemistry 28*, 6827−6835.
10. Rusnak, F., Sakaitani, M., Drueckhammer, D., Reichert, J., and Walsh, C. T. (1991) *Biochemistry 30*, 2916−2927.
11. Reichert, J., Sakaitani, M., and Walsh, C. T. (1992) *Protein Sci. 1*, 549−556.
12. Luke, R. K. J., and Gibson, F. (1971) *J. Bacteriol. 107*, 557−562.
13. Woodrow, G. C., Young, I. G., and Gibson, F. (1975) *J. Bacteriol. 124*, 1−6.
14. Lambalot, R. H., Gehring, A. M., Flugel, R. S., Zuber, P., LaCelle, M., Marahiel, M. A., Reid, R., Khosla, C., and Walsh, C. T. (1996) *Chem. Biol. 3*, 923−936.
15. Nahlik, M. S., Fleming, T. P., and McIntosh, M. A. (1987) *J. Bacteriol. 169*, 4163−4170.
16. Staab, J. F., and Earhart, C. F. (1990) *J. Bacteriol. 172*, 6403−6410.
17. Gill, S. C., and von Hippel, P. H. (1989) *Anal. Biochem. 182*, 319−326.
18. Lambalot, R. H., and Walsh, C. T. (1995) *J. Biol. Chem. 270*, 24658−24661.
19. Kleinkauf, H., and von Döhren, H. (1996) *Eur. J. Biochem. 236*, 335−351.
20. Gerngross, T. U., Snell, K. D., Peoples, O. P., Sinskey, A. J., Csuhai, E., Masamune, S., and Stubbe, J. (1994) *Biochemistry 33*, 9311−9320.
21. Bryce, G. F., and Brot, N. (1972) *Biochemistry 11*, 1708−1715.
22. De Crécy-Lagard, V., Marlière, P., and Saurin, W. (1995) *C. R. Acad. Sci., Ser. III 318*, 927−936.
23. Guilvout, I., Mercereau-Puijalon, O., Bonnefoy, S., Pugsley, A. P., and Carniel, E. (1993) *J. Bacteriol. 175*, 5488−5504.
24. Bearden, S. W., Fetherston, J. D., and Perry, R. D. (1997) *Infect. Immun. 65*, 1659−1668.
25. Tolmasky, M. E., Actis, L. A., and Crosa, J. H. (1993) *Infect. Immun. 61*, 3228−3233.
26. Drechsel, H., Stephan, H., Lotz, R., Haag, H., Zähner, H., Hantke, K., and Jung, G. (1995) *Liebigs Ann. Chem. 1995*, 1727−1733.
27. Chambers, C. E., McIntyre, D. D., Mouck, M., and Sokol, P. A. (1996) *BioMetals 9*, 157−167.
28. Jalal, M. A. F., Hossain, M. B., van der Helm, D., Sanders-Loehr, J., Actis, L. A., and Crosa, J. H. (1989) *J. Am. Chem. Soc. 111*, 292−296.
29. Keller, U. (1995) in *Genetics and Biochemistry of Antibiotic Production* (Vining, L. C., and Stuttard, C., Eds.) pp 173−196, Butterworth-Heinemann, Boston, MA.
30. Thibaut, D., Bisch, D., Ratet, N., Maton, L., Couder, M., Debussche, L., and Blanche, F. (1997) *J. Bacteriol. 179*, 697−704.
31. De Crécy-Lagard, V., Blanc, V., Gil, P., Naudin, L., Lorenzon, S., Famechon, A., Bamas-Jacques, N., Crouzet, J., and Thibaut, D. (1997) *J. Bacteriol. 179*, 705−713.
32. Keller, U., Kleinkauf, H., and Zocher, R. (1984) *Biochemistry 23*, 1479−1484.
33. Keller, U. (1987) *J. Biol. Chem. 262*, 5852−5856.
34. Keller, U., and Schlumbohm, W. (1992) *J. Biol. Chem. 267*, 11745−11752.
35. Stindl, A., and Keller, U. (1993) *J. Biol. Chem. 268*, 10612−10620.
36. Farrell, D. H., Mikesell, P., Actis, L. A., and Crosa, J. H. (1990) *Gene 86*, 45−51.

BI970453P